Nonlinear Plasmon-Photon Interaction Resolved by *k*-Space Spectroscopy

Nicolai B. Grosse, Jan Heckmann, and Ulrike Woggon
Institut für Optik und Atomare Physik, Technische Universität Berlin, Straße des 17. Juni 135, 10623 Berlin, Germany
(Received 20 December 2011; published 26 March 2012)

Metallic nanostructures support extreme localization and enhancement of optical fields via surface-plasmon (SP) resonances. Although SP are associated with giant enhancements of nonlinear phenomena such as second-harmonic generation (SHG), the role of SP in the process, whether as a field-enhancing catalyst or as a quasiparticle converted in the interaction, has remained experimentally elusive. We demonstrate how *k*-space spectroscopy can distinguish between the plasmonic and photonic SHG processes that occur in a metal nanofilm when it is optically driven via the Kretschmann geometry. The results revealed a nonlinear interaction where two SP annihilate to create a second-harmonic photon. This knowledge has implications for realizing the inverse process, plasmonic parametric down-conversion, which could act as a coherent source of entangled SP pairs.

DOI: 10.1103/PhysRevLett.108.136802 PACS numbers: 73.20.Mf, 42.65.Ky, 78.47.N−, 78.66.Bz

Because of their field-enhancement properties, surface plasmons (SP) can boost nonlinear optical phenomena while they remain bounded and propagate along a metal-dielectric interface. An excitation of SP is understood as a wave of electron displacements which is coupled to an electromagnetic wave having an evanescent form in both media. Further field confinement (even beyond the sub-wavelength regime) is possible on structured metal films, where SP become localized and find resonances. Indeed, this effect is the main driver of surface-enhanced Raman scattering (SERS) which has realized Raman spectroscopy at the single-molecule level [1]. While SERS is nonlinear to third-order, most contemporary technologies for the generation of quantum states of light and coherent frequency conversion rely on a second-order nonlinearity—the most elementary process being second-harmonic generation (SHG). In optical SHG, two photons at the fundamental frequency annihilate to produce a single photon at the second-harmonic frequency. Given that the probability of an event scales quadratically with the intensity of the fundamental field, it follows that structures which support SP-induced field enhancement also enhance SHG.

In their pioneering experiment, Simon *et al.* [2] observed an enhancement of SHG that was associated with SP excitation. They used a silver film which was optically coupled to a glass prism in the Kretschmann-Raether geometry [3]. From complementary studies of SHG in reflection from bulk metals, where SP were not involved, it has been established that the second-order nonlinear source must be located at the metal-dielectric interface [4], and that it is dominated by the quadrupolar response of the conduction electrons [5]. More recently, the localized SP that occur on metallic nanostructures have been shown to enhance SHG, thus allowing SHG to become a diagnostic for local field-enhancements (measured in the far field), and for measuring SP lifetimes via frequency mixing [6–10]. Amongst these experiments, there has been a trend for studying plasmonic structures of greater complexity, exhibiting very intricate effects. However, questions regarding the identification of the contributing elementary excitations to the nonlinear conversion process remain open.

In this Letter, we present experimental results that uncover the plasmon-photon nonlinear interactions which are responsible for the enhanced SHG from a metal nanofilm. What makes our approach distinctive is that we have revisited the pioneering experiments where SP propagate with well-defined *k* vectors on the surface of bulk metal; and that we have employed *k*-space spectroscopy in the Kretschmann geometry, to examine the emitted SHG in a way that provides precise information on SP nonlinear phase-matching. Because each type of nonlinear interaction conserves momentum, they can be distinguished by their unique signature in *k* space.

Our results show that the role of the surface-plasmon is not merely to provide a local field enhancement for driving SHG at the metal surface, but it is the fundamental SP themselves that are annihilated and convert into the second-harmonic photon. This knowledge not only has didactic value, but is the key to developing new structures that fully exploit SP nonlinearities. A striking example would be the inverse process to plasmon SHG, namely, parametric down-conversion, which could be a source of entangled SP pairs at compact length scales.

Hypothesis.—We propose that all permutations of surface plasmon (p) and photon (f) are allowed in the second-order nonlinear process of SHG, which can generate either p or f; and that each process can be identified by its condition for momentum conservation. The analysis is restricted to SP in the Kretschmann geometry, which comprises a glass prism coated with a metal film, exposed to air. We introduce the nonlinear phase-matching conditions for the set of SHG processes:

$$2k_f^{\omega}(\theta_{\rm in}) - k_f^{2\omega}(\theta_{\rm out}) = \Delta_{ff\text{-}f} \tag{1}$$

$$k_p^{\omega} + k_f^{\omega}(\theta_{\rm in}) - k_f^{2\omega}(\theta_{\rm out}) = \Delta_{pf\text{-}f} \tag{2}$$

$$2k_p^{\omega} - k_f^{2\omega}(\theta_{\rm out}) = \Delta_{pp\text{-}f} \tag{3}$$

$$2k_f^{\omega}(\theta_{\rm in}) - k_p^{2\omega} = \Delta_{ff\text{-}p} \tag{4}$$

$$k_p^{\omega} + k_f^{\omega}(\theta_{\rm in}) - k_p^{2\omega} = \Delta_{pf-p} \tag{5}$$

$$2k_p^{\omega} - k_p^{2\omega} = \Delta_{pp\text{-}p} \tag{6}$$

where k_p^{ω} and $k_p^{2\omega}$ are the k vectors of the SP for the fundamental ω and second-harmonic 2ω frequencies, where in the thick-film limit $k_p = k_0\sqrt{\epsilon_2\epsilon_3/(\epsilon_2+\epsilon_3)}$. Photon plane waves propagate into and out of the glass medium with angles $\theta_{\rm in}$ and $\theta_{\rm out}$ (to the normal) which project k-vector components parallel to the surface: $k_f^{\omega} = k_0(\epsilon_1^{\omega})^{1/2}\sin\theta_{\rm in}$ and $k_f^{2\omega} = 2k_0(\epsilon_1^{2\omega})^{1/2}\sin\theta_{\rm out}$ for $k_0 = \omega/c$. The media are described by their complex dielectric functions: glass ϵ_1, metal ϵ_2 of thickness d, and air ϵ_3 [11]. The so-called plasmon angle $\theta_{\rm sp}$ is defined as the angle for linear phase matching of the photon to the SP, by solving for $k_f = k_p$. This condition is commonly associated with an observation of attenuated total-internal reflection (ATIR). The nonlinear phase-matching conditions, as given by the Δ in Eqs. (1)–(6), were multiplied together and plotted in Fig. 1 as a gray scale map across $\theta_{\rm in}$ and $\theta_{\rm out}$. Momentum conservation for each nonlinear interaction (e.g., $\Delta_{ff\text{-}f} = 0$) thus appears as a dark line. Given that momentum conservation is a general requisite for strong SHG, it is anticipated that k-space measurements of SHG from a metal film will adhere to the dark lines, and therefore allow identification of the various plasmon-photon nonlinear interactions.

Because of SP hybridization, thin metal films support four modes of SP propagation: the symmetric bound s_b and leaky s_l; and the antisymmetric bound a_b and leaky a_l [12–14]. The modes are typically nondegenerate in their k vectors, which are found by solving the dispersion relation

$$\tanh(S_2 d)(\epsilon_1\epsilon_3 S_2^2 + \epsilon_2^2 S_1 S_3) + \epsilon_2 S_2(\epsilon_1 S_3 + \epsilon_3 S_1) = 0, \tag{7}$$

where $S_1^2 = k_p^2 - \epsilon_1 k_0^2$, $S_2^2 = k_p^2 - \epsilon_2 k_0^2$, and $S_3^2 = k_p^2 - \epsilon_3 k_0^2$, with the solution k_p complex. The modes a_b and a_l are not accessible via the Kretschmann geometry due to their large k_p. However, the symmetric modes are accessible, and also happen to possess field-enhancement localized to the metal-air interface. The k_p degeneracy for s_b and s_l is lifted as d is reduced or ϵ_2 is made lossy. The bound mode s_b (also known as the Brewster mode) has energy flow only into the metal, from both the air and glass media, and as such, is absorbed. Consequently, the excitation of s_b via a photonic plane wave is the cause for ATIR, which occurs at the s_b plasmon angle.

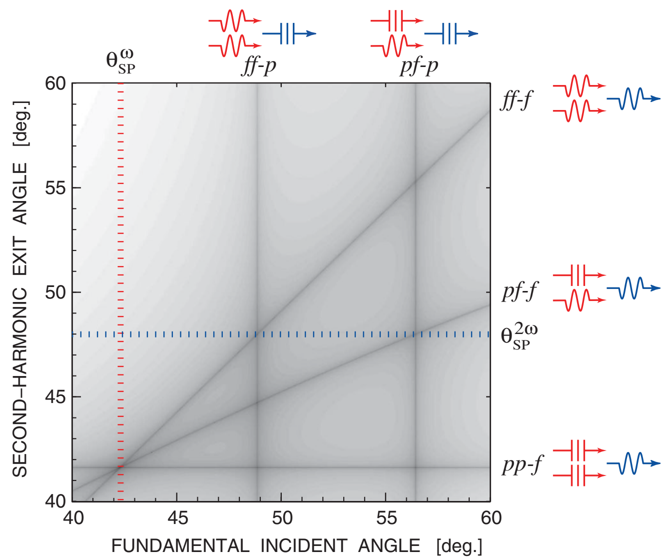

FIG. 1 (color). Feynman diagrams and nonlinear phase-matching conditions for surface plasmons (p) and photons (f) interacting for SHG. The solutions are mapped across the angles for the input fundamental (800 nm) and output second-harmonic (400 nm). Each interaction is identified by its own dark line. Dashed lines mark the angles $\theta_{\rm sp}$ for linear phase-matching between p and f. Calculation for pure silver on BK7 glass in the Kretschmann geometry (thick-film limit).

In contrast, the leaky mode s_l transports energy away from the metal, and into the glass. Unlike for the s_b mode, it is expected that only a fundamental field in the s_l mode, which drives a second-order polarization in the metal surface, will be able to radiate a second-harmonic field into the glass prism, and subsequently be detected. Henceforth, the solution to Eq. (7) for the fundamental s_l mode will be selected for k_p^{ω} as an ansatz for SP-induced SHG from the metal-air interface.

It is important to note that noble metals such as silver possess inversion symmetry for which SHG arises only from the surface. The source of second-order nonlinear polarization is proportional to $(\mathbf{E}^{\omega}\cdot\nabla)\mathbf{E}^{\omega}$ which is driven by the discontinuity of the fundamental electric field component normal to the surface [5]. Interestingly, Bloembergen *et al.* [15] predicted that two beams of SHG occur for the case of transmission into a medium; see Fig. 2(a). The inhomogenous second-harmonic (IH) is produced collinear with the fundamental (F), but after undergoing total-internal-reflection, is ultimately reflected with an angle offset due the dispersive media. The homogenous second-harmonic (H) does the converse. A key feature is that only IH has a contribution from the metal-air interface.

In summary, one expects to observe a background of photonic SHG in the IH and H beams, as manifested by the

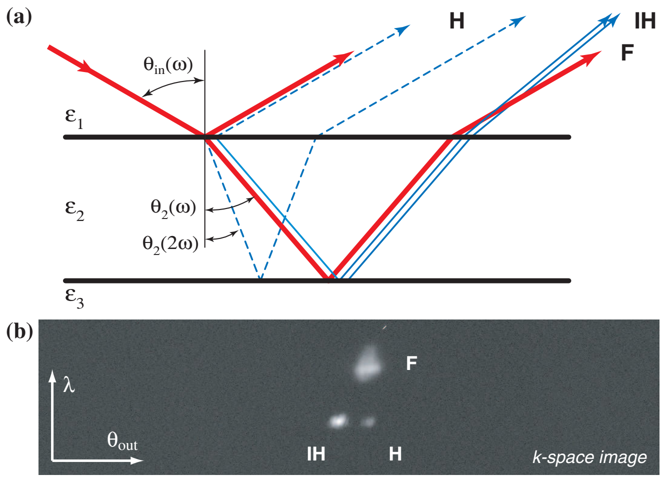

FIG. 2 (color). (a) Ray diagram of SHG from a three-layer system for which all media posses inversion symmetry. Illumination from the fundamental (F, thick line) produces the homogenous second-harmonic (H, dashed) which is collinear with F, while the inhomogenous second-harmonic (IH, thin line) exits with an offset angle. Note that only IH has a contribution from the outer interface. (b) Image delivered by the k-space spectrograph from the sample at $\theta_{\mathrm{in}}^{\omega} = 45.0°$ where F, H, and IH have been identified. (log of CCD counts in gray scale).

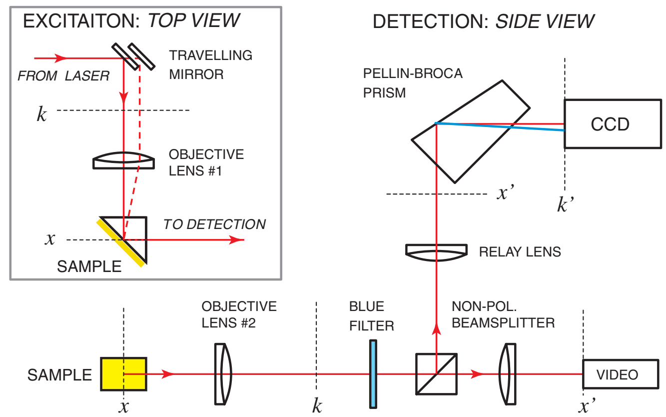

FIG. 3 (color online). The sample, a silver-coated prism, was illuminated by laser light at the angle for exciting SP, which then emitted second-harmonic light. The emitted light was filtered to balance the fundamental and second-harmonic optical powers. A relay lens imaged the back-focus of the objective to the CCD, thereby imaging k-space. A Pellin-Broca prism in the path ensured wavelength separation.

ff-f diagonal in Fig. 1, which is due simply to the intrinsic nonlinearity of the metal surfaces. However, a strong off-diagonal conversion, of a different origin, is expected to appear near the s_l plasmon angle, because of the availability of fundamental SP to drive the (radiative) plasmonic pp-f and pf-f interactions.

Experimental setup.—The k-space spectroscopic method delivered an intensity map of the light emitted by the sample as a function of exit angle and wavelength; see Fig. 3. By acquiring an image for each angle of the incident fundamental field, one could track the emitted second-harmonic light, and remap the intensity as a function of the incident and exit angles; see Fig. 4. Such a graph can then be compared with the nonlinear phase-matching diagram in Fig. 1.

The sample was based on a right-angled prism (BK7 glass) where a silver film had been applied on the hypotenuse side using vapor deposition (pressure 10^{-3} Pa, metal purity >99.9%). Atomic-force microscopy (AFM) revealed a 57 nm thick film with a subwavelength roughness of 2 nm and autocorrelation length 20 nm. Rather than rotating the sample, the input fundamental beam was displaced prior to focussing with an objective lens, with an identical lens placed in detection. A Gaussian beam radius of 190 μm at the sample position was chosen as a compromise between intensity and angular resolution (0.28°). Filters were employed in detection to suppress the fundamental and select the second harmonic. The light was relayed with a lens to a Pellin-Broca prism and CCD array (1024×256 elements). The relay lens projected the back-focus of the detection objective onto the CCD, where the long axis captured k-space information, and the short axis separated the wavelengths. The fundamental beam was derived from a Ti:sapphire laser (800 or 925 nm) with the pulse length set to 330 fs and repetition rate 76 MHz. Residual pump and second-harmonic were filtered out. The total detection efficiencies were estimated to be $\eta_\omega = 10^{-15}$ and $\eta_{2\omega} = 4 \times 10^{-2}$. Given the exposure time τ, and the CCD gain $g = 4.8$, the uncalibrated counts N can be converted into optical power using $P = \hbar\omega N/(\tau g \eta)$. The data were analyzed by programming virtual detectors to track and integrate the spots on the images, and also subtract background readings.

A typical image taken by the setup is shown in Fig. 2(b), where the sample was illuminated at an angle of 45.0° with 173 mW of 925 nm p-pol. Additional tests were performed with colored filters to determine the wavelengths of the spots on the image. We have identified spot F as the fundamental; H as the homogenous second-harmonic which was collinear with the fundamental at 45.0°; and IH as the inhomogenous second-harmonic which was emitted by the sample at 44.5°. Varying the input power from 20 to 320 mW revealed a linear response for F, and quadratic responses for H and IH. This confirms that H and IH were emitted via a second-order nonlinear process. Changing the input beam to s-pol at constant power caused H and IH to vanish. In s-pol, the lack of an electric field component normal to the surface denies the generation of SP and also annuls the quadrupolar source of nonlinearity at the metal surfaces. The SHG emission from the silver film sample was mapped in k-space using a high resolution angle scan of the incident fundamental field (wavelength 800 nm, power 86 mW, 241 steps, 10 s exposures). An integration of the recorded intensity was performed only in

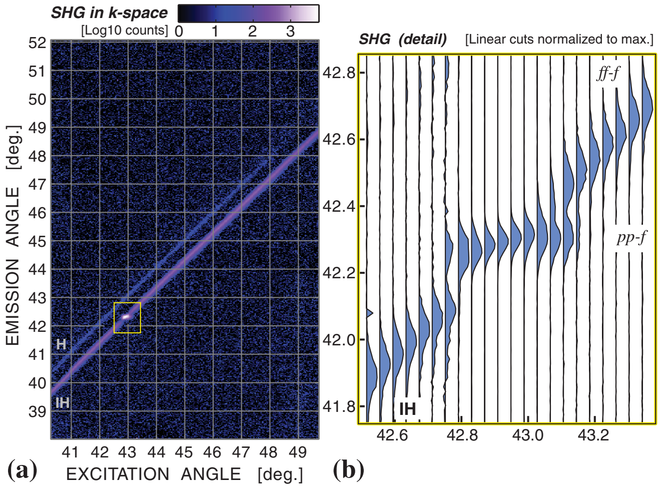

FIG. 4 (color). Revealing plasmon-photon nonlinear interactions. (a) High resolution k-space map of SHG obtained by exciting the silver sample using a fundamental at 800 nm scanned in angle. Counts integrated over the second-harmonic wavelength range and displayed in log scale (unsaturated). Weak H emission is visible as a diagonal, signifying ff-f optical SHG. The brighter IH, originating from the metal-air interface, is also diagonal but is displaced. (b) A detail of the SHG peak is plotted as a set of normalized cuts, showing the profile of the emitted beams (linear scale with shading). Visible is an off-diagonal component that remains fixed at an exit angle of 42.3°, thus identifying it as the pp-f nonlinear interaction for plasmon SHG.

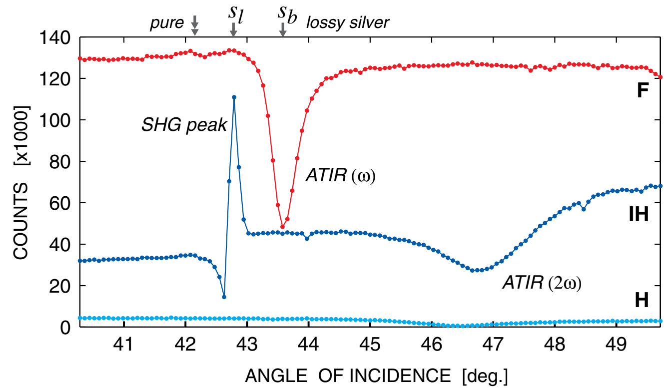

FIG. 5 (color online). Results showing that the SHG peak does not coincide with attenuated total-internal-reflection (ATIR) of the fundamental (F). Silver sample was scanned in angle with a fundamental beam at 925 nm. The broad dips in IH and H come from ATIR similar to F, but at the second-harmonic wavelength. The CCD counts were fully integrated while being tracked for each input angle. F is plotted with gain ×2 for clarity. Consideration of SP hybridization in lossy metal [17] can account for a separation of the SHG-peak and ATIR (ω) features.

wavelength around the second-harmonic, thereby preserving greater angular resolution.

Main result.—In Fig. 4(a), the strong IH adheres to an offset diagonal line $\theta_{\text{out}} = \theta_{\text{in}} - 0.7°$. The offset is caused by the dispersion of the glass and metal media. A weak H emission can be seen lying on a diagonal line $\theta_{\text{out}} = \theta_{\text{in}}$. Because both IH and H follow a diagonal, they originate from a purely photonic process (SHG via ff-f). However, the prominent spot in IH at $\theta_{\text{in}} = 43°$ displays elongation in the θ_{in} axis, which indicates a contribution other than the ff-f interaction. In Fig. 4(b), profiles along the θ_{out} axis were normalized to the maximum value in each curve. Near the corners of Fig. 4(b), IH follows the diagonal $\theta_{\text{out}} = \theta_{\text{in}} - 0.7°$, which comes from the ff-f interaction. However, there is a strong off-diagonal component that remains fixed at $\theta_{\text{out}} = 42.3°$. We offer an explanation with regard to Fig. 1. The off-diagonal component originates from the nonlinear interaction where two fundamental SP are converted into a second-harmonic photon (pp-f). Furthermore, our technique can be extended to probe the full gamut of interactions, far from the plasmon angle, by introducing an additional excitation that ensures a supply of fundamental SP.

Additional results.—By moving to a lower dispersion region (fundamental at 925 nm), absorption features for the second harmonic became accessible in the limited angle range. In Fig. 5, the beams F, H, and IH were tracked and integrated to get the optical power while the incident angle of the fundamental beam was scanned (173 mW, 121 steps, 20 s exposures). The IH curve shows a background contribution due to the ff-f interaction. A strong narrow peak is visible at 42.8° that is attributed to the excitation of SP in the s_l mode, where the SP have caused a local field enhancement at the air-metal interface and therefore boosted SHG. As identified earlier in the k-space maps, the interaction is pp-f. Adjacent to the peak is a sharp notch at 42.6° which is destructive interference between the source contributions from the glass-metal and metal-air interfaces. A broad minimum is visible in the background at 46.8°, which stems from ATIR for the s_b mode at 2ω. The H curve is bereft of peaks, having only a broad minimum at 46.5° due to a similar ATIR mechanism as in the IH mode. In the H source, there is no component generated at the metal-air interface. Hence, there can be no enhancement associated with the symmetric SP modes. The F curve shows a bold dip at 43.6°. This absorption feature is assigned to the ATIR effect arising when the s_b mode for ω is excited at its plasmon angle, thus delivering energy to the metal film wherein it is absorbed.

Upon comparing the F and IH results, it can be seen that the IH curve shows no deviation from background levels at the angle for the F dip. And at the angle for the IH peak, there is no increased absorption in F. Both of these features are clearly separated (by 0.8°). At first glance, this is a surprising result, given previous investigations which have stated that the SHG peak occurs at the same angle as the ATIR dip [2,16]. However, we argue that this is a natural outcome of SP hybridization, where the k-vector degeneracy for the bound and leaky symmetric modes is lifted when a metal film becomes thin and lossy. Vapor-deposited silver films are prone to surface roughness, oxidation and molecular adsorption. Because no precautions were taken in this regard, it is likely that our sample was exceptionally lossy [17]. Paradoxically, this has allowed us to witness the low loss excitation of a fundamental SP in the s_l mode (via SHG) which was separated from ATIR of the fundamental s_b mode. This result is of particular relevance to the technique of SP-resonance imaging, and for the incorporation of SP modes within photonic resonators.

Conclusion.—We have demonstrated how k-space spectroscopy can identify the combinations of elementary excitations (photons, surface plasmons) which contribute to nonlinear frequency conversion in metal surfaces. SHG was investigated from an optically excited metal nanofilm in the Kretschmann geometry. The results revealed an interaction where two surface plasmons annihilate to create a second-harmonic photon. Knowledge of the relevant nonlinear interactions that occur in nanometallic structures is vital for the development of applications in quantum plasmonics, such as subwavelength sources of entangled surface plasmons.

We acknowledge Chris Scharfenorth for preparation of the sample and Ronald Ries for the AFM measurements.

[1] K. Kneipp, Y. Wang, H. Kneipp, L. T. Perelman, I. Itzkan, R. R. Dasari, and M. S. Feld, Phys. Rev. Lett. **78**, 1667 (1997).

[2] H. J. Simon, D. E. Mitchell, and J. G. Watson, Phys. Rev. Lett. **33**, 1531 (1974).

[3] E. Kretschmann and H. Raether, Z. Naturforsch. A **23a**, 2135 (1968).

[4] F. Brown, R. E. Parks, and A. M. Sleeper, Phys. Rev. Lett. **14**, 1029 (1965).

[5] N. Bloembergen, R. K. Chang, S. S. Jha, and C. H. Lee, Phys. Rev. **174**, 813 (1968).

[6] T. Zentgraf, A. Christ, J. Kuhl, and H. Giessen, Phys. Rev. Lett. **93**, 243901 (2004).

[7] S. Palomba and L. Novotny, Phys. Rev. Lett. **101**, 056802 (2008).

[8] T. Hanke, G. Krauss, D. Träutlein, B. Wild, R. Bratschitsch, and A. Leitenstorfer, Phys. Rev. Lett. **103**, 257404 (2009).

[9] J. Renger, R. Quidant, N. van Hulst, and L. Novotny, Phys. Rev. Lett. **104**, 046803 (2010).

[10] T. Utikal, T. Zentgraf, T. Paul, C. Rockstuhl, F. Lederer, M. Lippitz, and H. Giessen, Phys. Rev. Lett. **106**, 133901 (2011).

[11] P. B. Johnson and R. W. Christy, Phys. Rev. B **6**, 4370 (1972).

[12] J. J. Burke, G. I. Stegeman, and T. Tamir, Phys. Rev. B **33**, 5186 (1986).

[13] K. L. Kliewer and R. Fuchs, Phys. Rev. **153**, 498 (1967).

[14] E. N. Economou, Phys. Rev. **182**, 539 (1969).

[15] N. Bloembergen and P. S. Pershan, Phys. Rev. **128**, 606 (1962).

[16] R. Naraoka, H. Okawa, K. Hashimoto, and K. Kajikawa, Opt. Commun. **248**, 249 (2005).

[17] Fundamental ATIR curve ($\lambda = 925$ nm) fitted to standard model [3] using $d = 57$ nm, $\epsilon_1 = 2.3$ and $\epsilon_3 = 1.0$ yielded $\epsilon_2 = -29 + 4.2i$; compare with $\epsilon_2 = -43 + 0.52i$ for pure silver [11]. Fit of SHG-peak and ATIR angles to modes s_l and s_b from [12] gives $\epsilon_2 = -12 + 8i$.